Journal of Molecular and Cellular Cardiology 80 (2015) 81–89

Contents lists available at ScienceDirect

Journal of Molecular and Cellular Cardiology

journal homepage: www.elsevier.com/locate/yjmcc

Original article

Ectopic automaticity induced in ventricular myocytes by transgenic overexpression of HCN2

Kensuke Oshita [a,b], Masayuki Itoh [a], Shingo Hirashima [c], Yoshihiro Kuwabara [d], Keiko Ishihara [a], Koichiro Kuwahara [d], Kazuwa Nakao [e,f], Takeshi Kimura [d], Kei-ichiro Nakamura [c], Kazuo Ushijima [b], Makoto Takano [a,*]

[a] Department of Physiology, Kurume University School of Medicine, Kurume, Japan
[b] Department of Anesthesiology, Kurume University School of Medicine, Kurume, Japan
[c] Division of Microscopic and Developmental Anatomy, Department of Anatomy, Kurume University School of Medicine, Kurume, Japan
[d] Department of Cardiovascular Medicine, Graduate School of Medicine, Kyoto University, Kyoto, Japan
[e] Medical Innovation Center, Graduate School of Medicine, Kyoto University, Kyoto, Japan
[f] Department of Medicine and Clinical Science, Graduate School of Medicine, Kyoto University, Kyoto, Japan

ARTICLE INFO

Article history:
Received 16 July 2014
Received in revised form 5 December 2014
Accepted 22 December 2014
Available online 3 January 2015

Keywords:
HCN2
Arrhythmia
Ion channel
Cardiomyocyte
Electrophysiology

ABSTRACT

Hyperpolarization-activated cyclic nucleotide-gated channels (HCNs) are expressed in the ventricles of fetal hearts but are normally down-regulated as development progresses. In the hypertrophied heart, however, these channels are re-expressed and generate a hyperpolarization-activated, nonselective cation current (I_h), which evidence suggests may increase susceptibility to arrhythmia. To test this hypothesis, we generated and analyzed transgenic mice overexpressing HCN2 specifically in their hearts (HCN2-Tg). Under physiological conditions, HCN2-Tg mice exhibited no discernible abnormalities. After the application of isoproterenol (ISO), however, ECG recordings from HCN2-Tg mice showed intermittent atrioventricular dissociation followed by idioventricular rhythm. Consistent with this observation, 0.3 μmol/L ISO-induced spontaneous action potentials (SAPs) in 76% of HCN2-Tg ventricular myocytes. In the remaining 24%, ISO significantly depolarized the resting membrane potential (RMP), and the late repolarization phase of evoked action potentials (APs) was significantly longer than in WT myocytes. Analysis of membrane currents revealed that these differences are attributable to the I_h tail current. These findings suggest HCN2 channel activity reduces the repolarization reserve of the ventricular action potential and increases ectopic automaticity under pathological conditions such as excessive β-adrenergic stimulation.

1. Introduction

Hyperpolarization-activated cyclic nucleotide-gated channels (HCNs) are widely expressed in a variety of tissues [1]. Among the four HCN subtypes (HCN1-4), HCN2 and HCN4 are abundantly expressed in the pacemaker cells of the sinoatrial node, where they generate a hyperpolarization-activated, nonselective cation current (I_f/I_h), which plays a key role in cardiac pacemaker activity [2]. HCN2 and 4 are also expressed in ventricular myocytes early during fetal development but are down-regulated at later stages [3,4].

As many as 50% of patients with heart failure die from sudden cardiac death, most likely caused by a lethal arrhythmia [5]. In heart failure and cardiac hypertrophy, the cardiac remodeling process reactivates ventricular myocardial expression of such fetal cardiac genes as HCN2 and HCN4 as well as CACNA1G and CACNA1H, which encode T-type Ca^{2+} channel subunits [6–8]. Although the mechanisms responsible for lethal arrhythmias in failing hearts remain unresolved, evidence suggests re-expression of fetal type cardiac ion channels contributes to the arrhythmogenicity. Indeed, when we generated transgenic mice that selectively expressed a dominant-negative neuron-restrictive silencer factor mutant in their hearts (dnNRSF-Tg mice), we found that these mice experienced sudden arrhythmic death and that there was a concomitant up-regulation of fetal type cardiac ion channels [9]. However, the contribution of each fetal cardiac channel to the arrhythmogenicity remains uncertain.

We previously reported that pharmacological blockade of HCN channels partially suppressed sudden arrhythmic death in dnNRSF-Tg mice [9]. We also carried out a preliminary analysis of transgenic mice overexpressing HCN2 in their hearts (HCN2-Tg) and reported that they were vulnerable to β-adrenergic-induced abnormal electrical activity [10]. In the present study, we carried out a detailed analysis of

* Corresponding author at: Department of Physiology, Kurume University School of Medicine, 67 Asahi-machi, Kurume 830-0011, Japan. Tel.: +81 942 31 7543; fax: +81 942 31 7728.
E-mail address: takanom@med.kurume-u.ac.jp (M. Takano).

http://dx.doi.org/10.1016/j.yjmcc.2014.12.019

the electrocardiographic and electrophysiological properties of single ventricular myocytes from HCN2-Tg mice. Our findings demonstrate that HCN2 channel activity reduces the repolarization reserve of the ventricular action potential (AP) and increases the ectopic automaticity of ventricular myocytes.

Preliminary results from this study were communicated at the annual meeting of the Japanese Physiological Society (Tokyo 2013) and at the Congress of the International Union of the Physiological Society (Birmingham 2013) [11].

2. Materials and methods

All animal experiments were approved in advance by the Animal Ethics Committee of Kurume University (No. 23-11). Animal care and experiments conform to the Guidelines for the Care and Use of Laboratory Animals published by the US National Institutes of Health (NIH Publication No. 85-23, revised 1996).

2.1. Experimental animals

We overexpressed mouse HCN2 cDNA in the hearts of C57BL/6 mice using the α-MHC promoter (HCN2-Tg) [10]. HCN2-Tg and their wild-type (WT) littermates were used while they were between 10 and 14 weeks of age.

2.2. Cell isolation

After deeply anesthetizing mice using 3.0% sevoflurane, their hearts were quickly removed and the ventricular myocytes were isolated through collagenase digestion [12].

2.3. Heterologous expression experiment

Mouse HCN2 cDNA was subcloned into pCDNA3 vector, which was then transfected into CHO cells using Attractene (QIAGEN). Electrophysiological studies were carried out 2 days after the transfection.

2.4. Electrophysiological measurements

APs and membrane currents were recorded from ventricular myocytes using ruptured and perforated whole-cell patch clamp methods. The composition of the pipette solutions and the bathing solutions are available in the on-line data supplement. All the experiments were carried out at 33–35 °C.

2.5. Quantitative RT-PCR analysis

Levels of mouse HCN1 (TaqMan assay ID: Mm00468832_m1), HCN2 (Mm00468538_m), HCN3 (Mm01212852_m1), HCN4 (Mm01176086_m1), Kir2.1 (Mm00434616_m1), Cav1.2 (Mm01188822_m1), Kv4.2 (Mm00807577_m1), Kchip2 (Mm00518915_g1) and Kv11.1 (Mm01161732_m1) mRNA were determined using quantitative real-time RT-PCR (qPCR) in predesigned TaqMan Gene Expression Assays (Applied Biosystems, Inc.). Relative levels of mRNA were normalized to the level of 18S rRNA.

2.6. ECG recording

Mice were anesthetized using 2.0% sevoflurane and placed in a supine position on a warming plate to maintain body temperature at around 37 °C. Two-lead ECGs (lead I, lead II) were recorded and analyzed using a PowerLab Data Acquisition System with LabChart software (AD Instruments Inc.). Vector ECGs were reconstructed using lead I and lead aVF. Lead aVF was calculated using following equation:

$$\text{lead aVF} = \frac{1}{\sqrt{3}} \times (2 \times \text{lead II} - \text{lead I})$$

2.7. Fluorescence immunohistochemistry

Mice were anesthetized with 3% sevoflurane and perfused through the left ventricle with heparinized saline followed by 4% paraformaldehyde in PBS. The hearts were removed and post-fixed for 2 h with 4% paraformaldehyde, cryoprotected for 18 h in 30% sucrose, and mounted in OCT Embedding Compound (Sakura Finetek, Japan), after

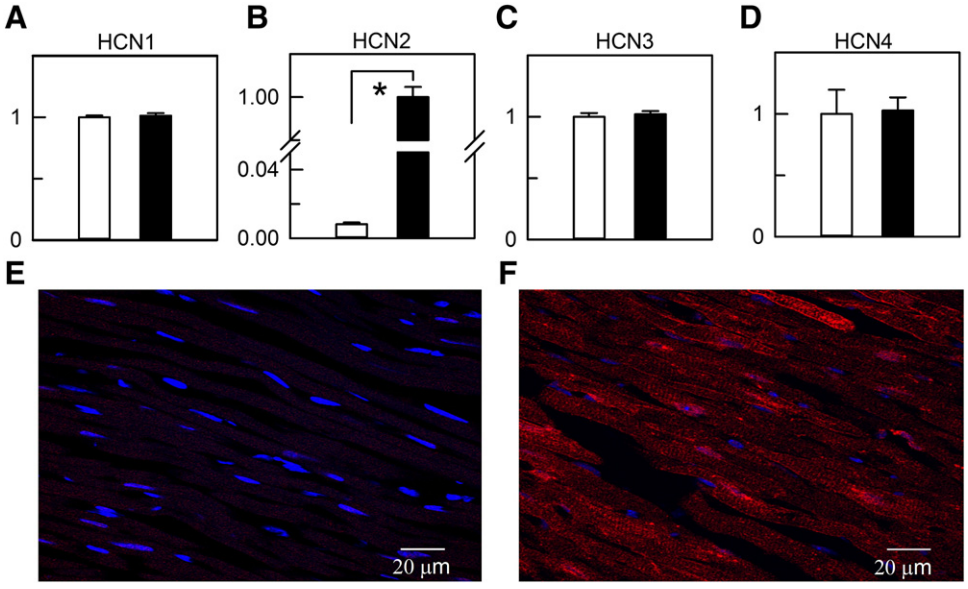

Fig. 1. Expression levels of HCN subtypes in the ventricles of HCN2-Tg mice (A–D) qPCR analysis of the relative mRNA level of HCN family proteins in ventricles from WT (white bars, $n = 5$) and HCN2-Tg (black bars, $n = 5$) mice. Note that the expression level of HCN2 mRNA is significantly higher in HCN2-Tg than WT hearts ($p < 0.01$). (E, F) Immunohistochemical staining for HCN2 demonstrating the subcellular localization of HCN2 in WT (E) and HCN2-Tg (F) ventricles. Nuclei were stained blue with DAPI. Bars represent 20 μm.

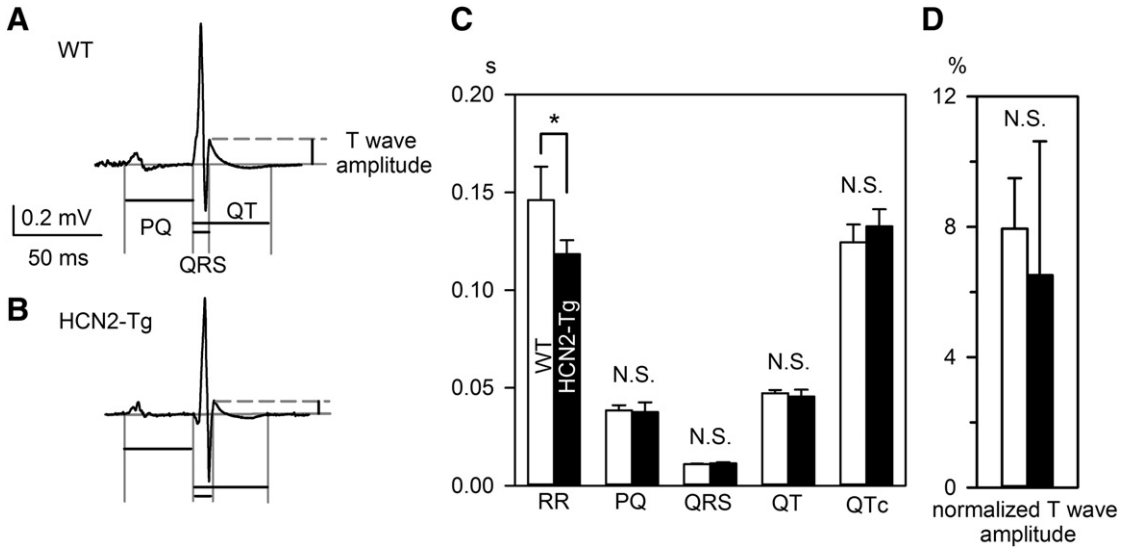

Fig. 2. ECG parameters in WT and HCN2-Tg mice (A, B) Representative ECG traces in WT (A) and HCN2-Tg (B) mice. Definitions of the PQ, QRS and QT intervals and the T-wave amplitude are indicated. (C) ECG parameters in WT (white bars, $n = 5$) and HCN2-Tg (black bars, $n = 5$) mice. In HCN2-Tg mice, RR intervals were significantly shorter than in WT mice. Other parameters (PR interval, QRS interval, QT interval, QTc (Bazett's Formula)) did not significantly differ between WT and HCN2-Tg mice. (D) Relative T-wave amplitudes in WT (white bar) and HCN2-Tg (black bar) mice.

which serial 5-μm sections were cut with a cryostat (CM3050S, Leica Microsystems, Wetzlar, Germany). The tissue sections were washed in PBS and then blocked with 5% normal goat serum (NGS) in PBS containing 0.05% Triton X-100. Thereafter, the sections were incubated with a polyclonal rabbit anti-HCN2 antibody (1:1000 dilution, Alomone Labs, Jerusalem, Israel) for 1 day at 4 °C, followed by incubation with Alexa Fluor 568 goat anti-rabbit IgG (1:2000 dilution, Invitrogen, Carlsbad, CA) for 2 h at room temperature. Images were captured using a Fluoview 1000 laser-scanning confocal microscope system (Olympus, Tokyo, Japan).

2.8. Statistical analysis

Data are shown as mean ± SD. Repeated-measures one-way analysis of variance (ANOVA) followed by the Tukey test and the Student's *t*-

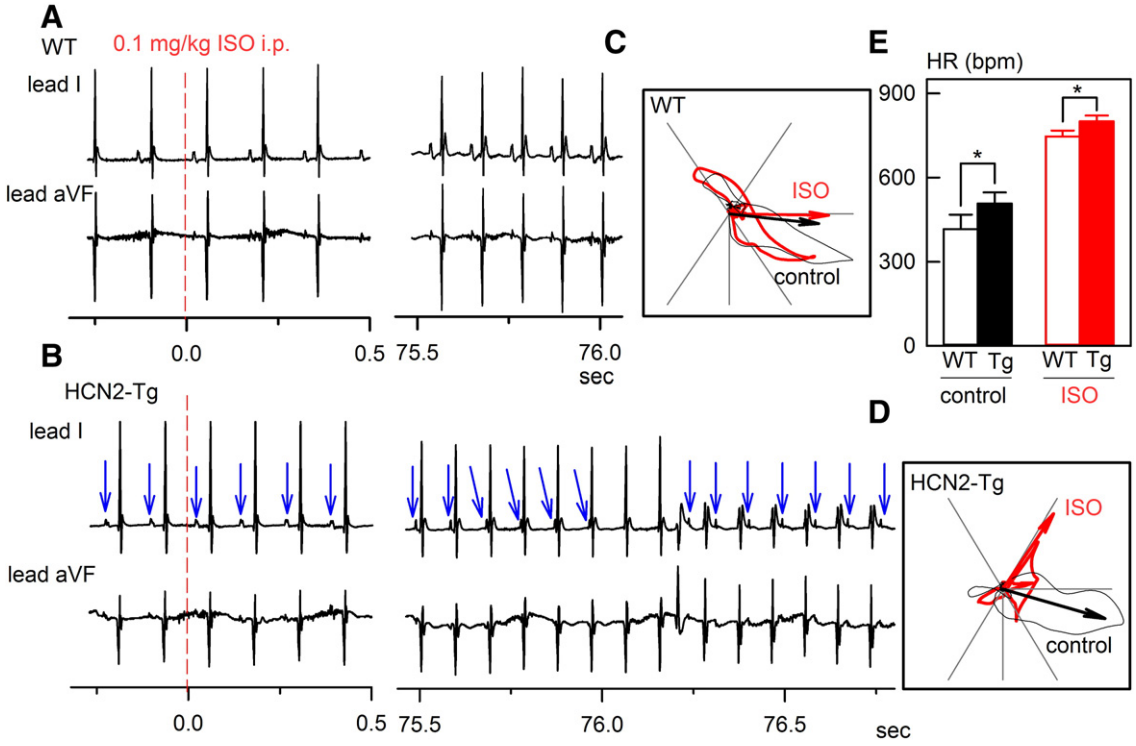

Fig. 3. Idioventricular rhythm induced by ISO in HCN2-Tg mice (A, B) Representative ECG traces in WT (A) and HCN2-Tg (B) mice. Under control conditions, we observed no arrhythmias in WT or HCN2-Tg mice. ISO (0.1 mg/kg) was intraperitoneally injected at 0 s. Note that in HCN2-Tg mice the ECG trace showed atrioventricular dissociation followed by idioventricular rhythm. The blue arrows indicate P waves to emphasize the AV dissociation. (C) Representative vector ECG in WT mice before (black) and after (red) ISO application. (D) Representative vector ECG in HCN2-Tg mice. ISO induced ectopic ventricular rhythm in HCN2-Tg hearts. (E) Heart rates in WT (open bar) and HCN2-Tg (filled bar) mice before (black) and after (red) ISO administration. With or without ISO, heart rates in HCN2-Tg mice were significantly faster than in WT mice.

test were used for data analysis. Differences were considered significant when $p < 0.05$.

3. Results

3.1. Isoproterenol (ISO) induces idioventricular rhythm in HCN2-Tg mice

Recent studies suggest that in addition to HCN2, HCN1 and HCN3 may also be involved in generating murine ventricular APs [13,14]. We therefore first examined whether the expression of these channels was altered in HCN2-Tg myocytes. qPCR experiments showed that there were no secondary changes in the expression of HCN1, HCN3 or HCN4 in HCN2-Tg myocytes. On the other hand, HCN2 expression was >100 times higher in HCN2-Tg than WT myocytes (Figs. 1A–D). Immunostaining confirmed that virtually no HCN2 was present in WT ventricular ventricles. In HCN2-Tg hearts, however, HCN2-immunoreactivity was ubiquitous throughout the ventricle (Fig. 1F).

Free moving, telemetric ECG records from HCN3 knockout mice ($HCN3^{-/-}$) revealed significant changes in the waveform: the QT interval was prolonged at lower heart rates in $HCN3^{-/-}$ mice, and the amplitude of the T-wave was greater [14]. By contrast, the only significant change in the ECG waveform in HCN2-Tg mice was a shortening of the RR interval (Fig. 2). The relative amplitude of the T-wave (normalized to the amplitude of the R-wave) varied considerably, and there was no significant difference between the WT ($7.9 \pm 1.5\%$, $n = 5$) and HCN2-Tg ($6.5 \pm 4.1\%$, $n = 5$, $p = 0.49$) hearts.

We previously reported that β-adrenergic stimulation increased the occurrence of ventricular arrhythmias during telemetric recording of ECGs in HCN2-Tg mice [10]. To explore the mechanism of this arrhythmia, we carried out electrocardiographic vector analysis under general anesthesia [15]. In WT mice, the intraperitoneal application of ISO (0.1 mg/kg) simply induced sinus tachycardia; no ventricular arrhythmias were observed, and the polarity of the QRS complex and the morphology of the vector loop were not significantly changed. By contrast, ISO-induced atrioventricular dissociation in HCN2-Tg mice, followed by idioventricular rhythm (Fig. 3B). These ventricular rhythms occurred intermittently and returned to sinus rhythm when the AV dissociation disappeared. Vector ECG revealed that upward vector loop and left

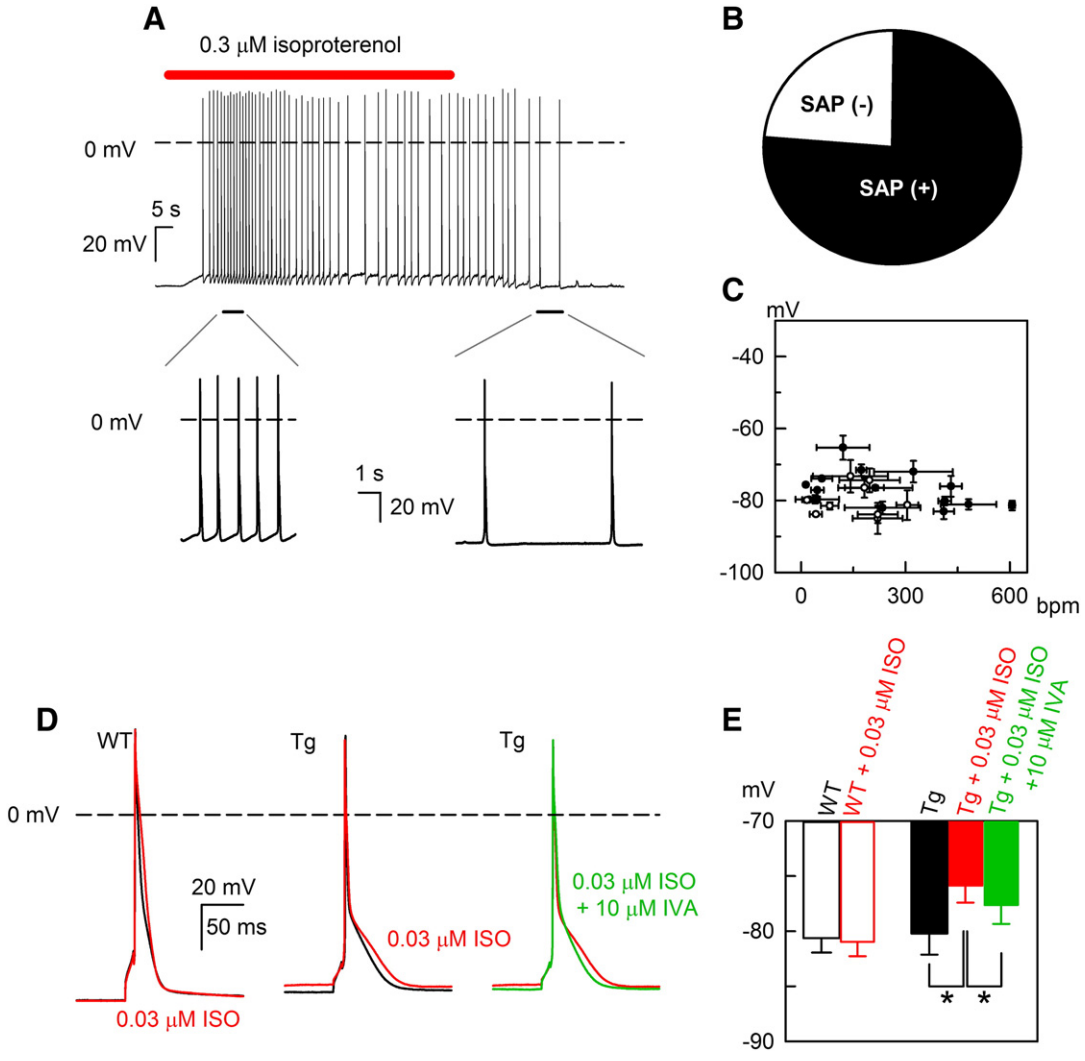

Fig. 4. ISO-induced SAP in HCN2-Tg myocytes (A) Continuous trace of a current-clamp recording from an HCN2-Tg myocyte. In this experiment, the membrane potential was recorded using the perforated patch method. The application of 0.3 μmol/L ISO is indicated by the red bar. (B) Fractions of ISO-treated HCN2-Tg myocytes with and without SAPs. The black sector indicates the percentage of myocytes exhibiting SAPs (76%). (C) Scatter plot of MDPs and firing rates (beats per min; bpm) of SAPs in ISO-treated HCN2-Tg myocytes: white symbols, data recorded using the perforated whole-cell patch method; black symbols, ruptured whole-cell patch method. Firing rates were calculated by successively averaging the inter-AP intervals in trains of SAPs; inter-AP intervals were measured from the onset of SAPs to the termination of ISO application. (D) Representative induced AP waveform in WT (left) and HCN2-Tg (center, right) myocytes. In HCN2-Tg, depolarization of RMP was observed at even lower concentration (0.03 μmol/L ISO). It should be noted that 10 μmol/L ivabradine significantly reversed the depolarization. In WT, ISO (red line) neither induced depolarization of RMP nor SAP. (E) RMPs in WT myocytes (open bars, $n = 6$) and in HCN2-Tg myocytes (filled bars, $n = 10$); control, black bars; with ISO, red bars; with ISO and IVA, green bar (repeated-measures one-way ANOVA followed by Tukey test, $^*p < 0.05$).

axis deviation were consistently induced during the idioventricular rhythm (Fig. 3D). These findings suggest that ISO increased ectopic pacemaker activity in the ventricles of HCN2-Tg hearts (Figs. 3A, C).

3.2. ISO induces depolarization and spontaneous APs in HCN2-Tg myocytes

To obtain insight into the cellular mechanism underlying the ectopic ventricular rhythm in HCN2-Tg mice, we recorded the membrane potentials of HCN2-Tg myocytes using pipette solution containing 5 mmol/L EGTA. As shown in Fig. 4A, the application of 0.3 μmol/L ISO depolarized the resting membrane potential (RMP) and often induced an irreversible train of spontaneous APs (SAPs); i.e., SAPs were observed in 76% of cells tested (32 of 42 cells, Fig. 4B). Fig. 4C summarizes the relationship between the average firing rates and the maximal diastolic potentials (MDPs) of SAPs in HCN2-Tg myocytes. The white symbols depict the values recorded in the perforated whole-cell patch experiments ($n = 9$), while the black symbols represent those recorded in the ruptured whole-cell patch experiments. However, the occurrence of SAPs did not differ between the experimental configurations. Twenty-four percent of ventricular myocytes isolated from HCN2-Tg hearts, ISO depolarized the RMP, but did not induced SAPs (data not shown). It was recently reported that HCN2 channel possessed permeability to Ca^{2+}, as well as Na^+ and K^+, which may induce delayed after depolarization (DAD) [16]. To test this possibility, we carried out fast pacing of HCN2-Tg myocytes. As shown in Supplementary Fig. 1, DAD was not induced both in the presence and absence of ISO, when recorded with 5 mmol/L EGTA pipette solution. These findings suggested that intracellular Ca^{2+}-dependent mechanism may not be involved in this automaticity.

In HCN2-Tg myocytes, ISO depolarized RMP even at lower concentration; 0.03 μmol/L ISO depolarized RMP from -80.2 ± 1.9 mV to -75.9 ± 1.6 mV (Fig. 4E, $n = 10$, $p < 0.05$). The depolarization of RMP was significantly reversed by the application of HCN channel blocker, ivabradine from -75.9 ± 1.6 mV to -77.6 ± 1.7 mV (Fig. 4E, $n = 10$, $p < 0.05$). In WT myocytes, ISO neither induced SAPs (data not shown) nor depolarized the RMP (Fig. 4D, left panel), which were -80.6 ± 1.3 mV and -81.0 ± 1.3 mV in the absence and presence of 0.03 μmol/L ISO, respectively (Fig. 4E, $n = 6$). ISO (0.3 μmol/L) also failed to induce SAP or depolarization in WT myocytes (data not shown).

To clarify the mechanisms underlying ISO-induced depolarization and SAPs, we next evaluated the membrane currents that contribute to the RMP. As shown in the right panel of Fig. 5A, inhibition of I_{K1} using 1 mmol/L Ba^{2+} unmasked a time-dependent inward current activated by hyperpolarizing pulses (i.e., I_h) in HCN2-Tg myocytes. In WT cells, I_h was negligibly small or absent when the K^+ concentration in the bathing solution was within the physiological range (Fig. 5A, left panel). The current–voltage (I–V) relationships for I_h (open circles) and the background current (filled circles) are shown in Fig. 5D.

We also compared the amplitudes of the inward-rectifier K^+ current (I_{K1}) measured as a Ba^{2+}-sensitive component. The I–V relationships in Fig. 5B show that I_{K1} density did not significantly differ between WT (open triangles) and HCN2-Tg (filled triangles) myocytes. Consistent with this observation, qPCR revealed that levels of Kir2.1 mRNA also did not significantly differ between WT and HCN2-Tg myocytes (Fig. 5C).

To determine whether I_h could be activated at membrane potentials close to the MDP or depolarized RMP in HCN2-Tg myocytes, we analyzed voltage-dependent, steady-state I_h activation curves before and after the application of ISO (Fig. 5E). We used a 2-step pulse protocol, in which conditioning pulses (to −50 and to −150 mV for 1250 ms) were followed by a test pulse to −150 mV, as shown in the upper panel of Fig. 5A. The amplitudes of the time-dependent components at the onset of test pulse were normalized as %activation and plotted. We then fitted the Boltzmann equation to each data set: $\%\text{activation} = 1/(1 + \exp((V_m - V_{1/2})/s))$, where $V_{1/2}$ is the membrane potential at which activation is half-maximal, V_m is the membrane potential, and s is the slope factor. It is clear from Fig. 5E that $V_{1/2}$ was shifted from -118.5 ± 2.9 mV to -90.2 ± 1.5 mV by ISO application ($n = 4$, $p < 0.01$). These activation curves suggest that under control conditions 7% of I_h is activated at RMP, whereas in the presence of ISO as much as 25% of I_h is activated at the MDP (-77.1 ± 4.7 mV) of SAPs.

Finally, we compared the time course of the diastolic depolarization of SAPs and the activation time course of I_h in HCN2-Tg myocytes (Fig. 5F). As indicated by the dashed lines, the activation kinetics of I_h at −80 mV were so fast that the current could be sufficiently activated

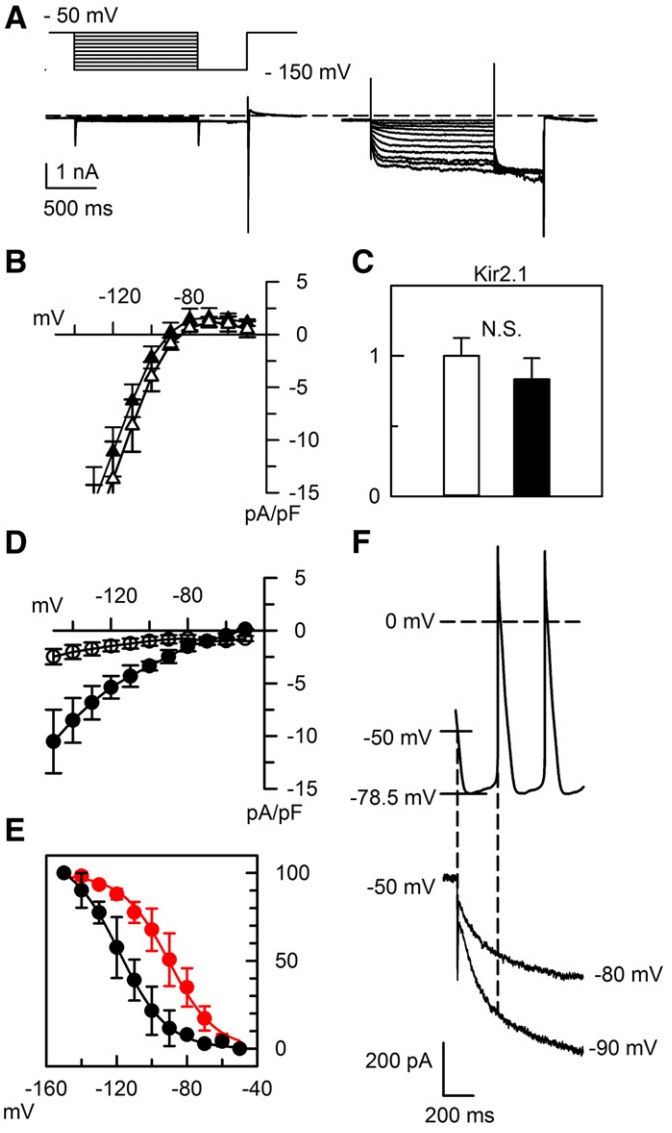

Fig. 5. Shift of the I_h activation curve underlies the depolarization of RMP in HCN2-Tg myocytes. (A) Representative current traces recorded from WT (left) and HCN2-Tg (right) myocytes after the application of 1 mmol/L Ba^{2+}. A robust I_h was revealed after complete inhibition of I_{K1}. The pulse protocol is indicated above the traces. (B) I–V relationship for I_{K1} in WT (open triangles) and HCN2-Tg (filled triangles) myocytes. I_{K1} amplitude was measured as the Ba^{2+}-sensitive component. (C) qPCR analysis of the relative levels of Kir2.1 mRNA in WT (open bar) and HCN2-Tg (filled bar) hearts ($n = 5$ in each group). (D) I–V relationship for I_h in HCN2-Tg myocytes (filled circles) in the presence of 0.3 μmol/L ISO. The amplitude of the time-dependent component during the conditioning pulse was measured as I_h and normalized to the cellular membrane capacitance. In WT myocytes, only the time-independent background current was observed (open circles). (E) Voltage-dependent steady-state activation curve for I_h in the presence (red circles) and absence (black circles) of 0.3 μmol/L ISO. (F) Upper panel shows an expanded SAP trace. The MDP was −78.5 mV, and the peak-to-peak interval was 209 ms. The lower panel shows the time course of I_h activation in HCN2-Tg myocytes at −80 and −90 mV. The membrane current was recorded in bathing solution containing 1 mmol/L Ba^{2+} and 0.3 μmol/L ISO.

at MDP during the beat-to-beat intervals between SAPs. This strongly suggests that in HCN2-Tg myocytes, ISO-induced depolarization of RMP and diastolic depolarization of SAPs are due to ISO-induced activation of HCN2.

3.3. Repolarization reserve in HCN2-Tg myocytes

Fenske et al. [14] recently reported detecting faint expression of HCN3 in ventricular myocytes from adult mice. They also reported that in HCN3 knockout ($HCN3^{-/-}$) mice, AP duration (APD) was shortened along with alteration of T-wave amplitude on ECGs. We therefore used ruptured whole-cell patch methods to evaluate the shape of APs induced in HCN2-Tg myocytes.

In Fig. 6A, AP was recorded in the absence of ISO. The black and red lines indicate APs of WT and HCN2-Tg, respectively. As summarized in Fig. 6C, the amplitude of action potential (APA) was not significantly different between HCN2-Tg and WT myocytes. AP duration at 90% repolarization (APD_{90}) was significantly longer, whereas APD_{50} and APD_{20} were significantly shorter in HCN2-Tg myocytes. Fig. 6B depicts the AP waveforms recorded in the presence of 0.3 μmol/L ISO. APs were induced in the same cells as in Fig. 6A. In HCN2-Tg myocyte, the RMP was depolarized due to the activation of HCN2. At the same time, and the amplitude of overshoot was reduced, most probably due to the inactivation of voltage-gated Na^+ current at depolarized RMP. Action potential parameters are summarized in Fig. 6C; APA was significantly smaller in HCN2-Tg. The differences of APD_{90}, APD_{50}, and APD_{20} were even more apparent in the presence of ISO.

At the given composition of the intra- and extracellular solutions, predicted reversal potential of I_h was −35 mV. During repolarization phase, it is therefore anticipated that outward tail current of I_h shortened APD at the membrane potentials more positive than −35 mV, and inward tail current of I_h prolonged APD at the membrane potentials more negative than −35 mV. To test this idea, we carried out AP clamp experiments in CHO cells expressing mouse HCN2 cDNA. We used CHO cells because they do not express voltage-gated K^+ currents, and it was easy to isolate I_h tail currents from the background current. We first activated I_h using a square pulse protocol with high-K^+ pipette solution containing 1 mmol/L cAMP (Fig. 7A). It should be noted that the direction of the tail current reversed between −40 and −30 mV. When we then perfused 5.4 mmol/L K^+, 10 mmol/L Cs^+ bathing solutions, inward I_h was almost completely blocked, but the outward tail current was less sensitive to this solutions.

In the same cell, we activated I_h using a command pulse shaped like an AP sampled from an HCN2-Tg myocyte in the presence of ISO (Fig. 7B, inset). In the left panel of Fig. 7B, the black line was recorded in the control bathing solution, the green line in the 5.4 mmol/L K^+, 10 mmol/L Cs^+ bathing solution. It is clear that a Cs^+-sensitive component was recorded during all phases of the AP. In the right panel of Fig. 7B, the *I–V* relationship was obtained from the repolarization phase in the AP clamp experiment ($n = 6$). The intersections between black line and magenta line show that the reversal potential of the Cs^+-sensitive component was close to −35 mV. It is evident from these results that the I_h tail current could participate in the repolarization phase of the mouse ventricular AP.

Finally, we confirmed that the expression of ion channels that could potentially affect APD was unchanged in HCN2-Tg myocytes. qPCR analyses showed that the expression of Cav1.2, Kv11.1, Kv4.2 and Kchip2 did not significantly differ between WT and HCN2-Tg myocytes. Furthermore, we detected no secondary changes in the densities of L-type Ca^{2+} currents and 4-AP-sensitive transient outward currents in HCN2-Tg myocytes (Supplementary Fig. 2).

4. Discussion

Evidence from numerous studies is suggestive of the potential arrhythmogenicity of HCNs in failing hearts but much remains unclear. For example, HCN2 and HCN4 are up-regulated in hypertrophied rat hearts and in the human failing heart [8,17,18]. In the mouse transverse aortic constriction (TAC) model, however, the amplitude of I_h is significantly increased, but there is a concomitant up-regulation of only HCN1

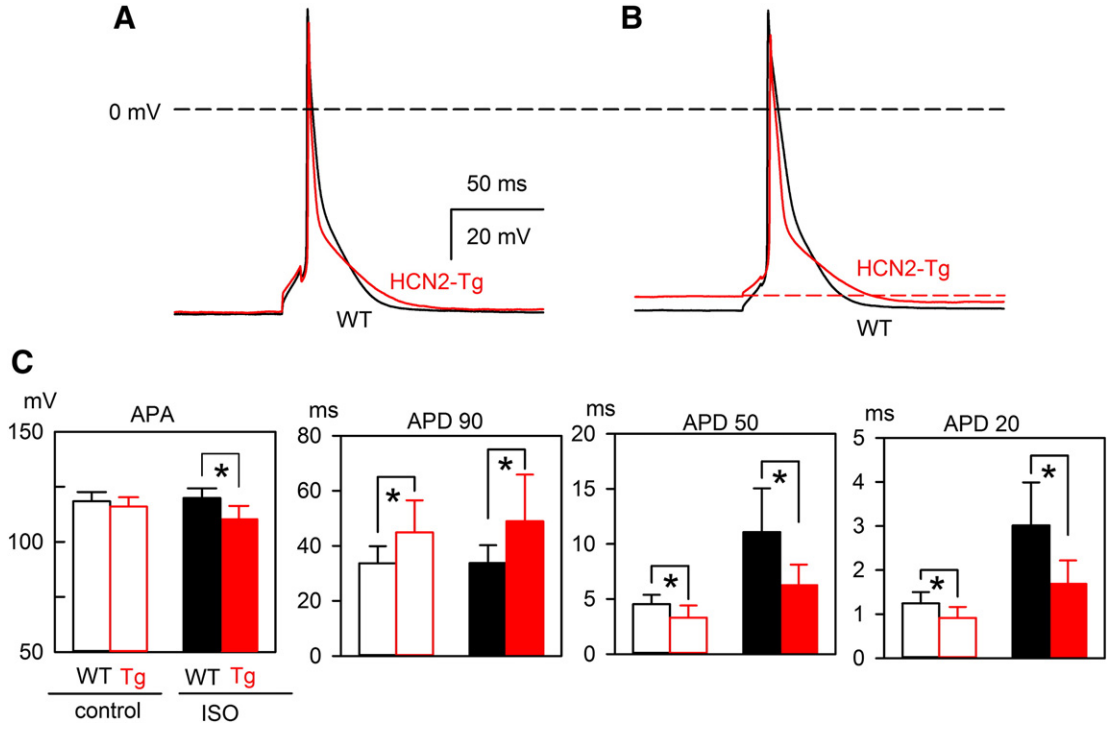

Fig. 6. Action potential parameters of induced APs (A) Representative AP traces of WT (black line) and HCN2-Tg myocyte (red line) under control condition. (B) AP traces in the presence of 0.3 μmol/L ISO. Black and red lines, same as in (A). As emphasized by the red dash line, depolarization of RMP was observed only in HCN2-Tg myocytes. (C) Summaries of APA, APD_{90}, APD_{50}, APD_{20}: black bars, WT; red bars, HCN2-Tg; open bars, without ISO; filled bars, with 0.3 μmol/L ISO. Bars depict means ± S.D., $^*p < 0.05$.

expression; expression of HCN2 and HCN4 is unaffected [13]. Moreover, none of the animal models of cardiac hypertrophy develop lethal arrhythmias. On the other hand, transgenic mice overexpressing a dominant-negative neuron-restricted silencing factor mutant (dnNRSF-Tg) die from ventricular tachyarrhythmia [9]. In the dnNRSF-Tg ventricle, robust increases in the expression of fetal cardiac channels, including HCN2 and HCN4 as well as CACNA1G and CACNA1H, two T-type Ca^{2+} channel subunits, have been reported [9], and blockade of HCN channels using ivabradine was recently shown to improve survival among dnNRSF-Tg mice [10]. This result is consistent with the potential arrhythmogenicity of HCN channels. It appears, however, that the overexpression of CACNA1G does not, by itself, provoke arrhythmias or SAPs in mouse ventricular myocytes; it only increases Ca^{2+} transients and induces mild cardiac hypertrophy [19]. Likewise, we showed that the overexpression of HCN2 is not, by itself, sufficient to induce lethal arrhythmia, but it induced an idioventricular rhythm under excessive β adrenergic stimulation. DADs are frequently observed in the myocytes isolated from hypertrophied heart. However, as shown in the present study, DADs were not induced by the overexpression of fetal type cardiac channels. These result suggested that the mechanism of ectopic automaticity in HCN2-Tg may be fundamentally different from that in hypertrophied heart.

In the present study, β-adrenergic stimulation consistently depolarized the RMP of HCN2-Tg myocytes. However, the magnitude of the depolarization did not directly correlate with the occurrence of SAPs, as depolarized RMPs in quiescent HCN2-Tg myocytes did not significantly differ from the MDPs of the SAPs. Why some cardiac myocytes (76%) exhibited SAPs while others (24%) did not remains unclear. In studies attempting to generate a "biological pacemaker" by overexpressing HCN2 in ventricular myocytes, the simultaneous overexpression of voltage-gated Na^+ channels (SkM1) was required for stable firing of SAPs [20]. This suggests, cell-to-cell variation in I_{Na} density may determine whether or not HCN2-Tg myocytes exhibit SAPs. In addition, I_{Na} and the T-type Ca^{2+} current ($I_{Ca\text{-}T}$) are activated at a similar range of membrane potentials [21]. Thus, the simultaneous overexpression of $I_{Ca\text{-}T}$ and I_h might induce stable SAPs in transgenic model mice and in hypertrophied hearts.

The firing rates of SAPs in HCN2-Tg myocytes were much less than 600 bpm. Because the heart rates of mice can easily increase to more than 700 bpm during β-adrenergic stimulation, the automaticity of HCN2-Tg ventricular myocytes may be masked by physiological pacing mediated via the cardiac conduction system [22,23]. Indeed, in this study ISO-induced ectopic ventricular rhythm in HCN2-Tg mice consistently preceded AV dissociation. Under physiological conditions, the pacemaker activity of the SA node might overdrive the idioventricular rhythm.

The repolarization phase of ventricular APs is primarily governed by activation of multiple K^+ currents, including I_{to}, the fast- and slow delayed rectifier K^+ currents (I_{Kr} and I_{Ks}; also known as HERG and KVLQT1), and I_{K1} [24–27]. This redundancy of repolarizing currents is called the "repolarization reserve" [28]. In the present study, we showed that when APs were recorded using the ruptured whole-cell patch method, the transgenic overexpression of HCN2 in mouse ventricular myocytes reduced the repolarization reserve and prolonged APD at the membrane potentials more negative than −35 mV. These results appear to be consistent with the observations reported in $HCN3^{-/-}$ myocytes, although the changes in APD were in the opposite direction in HCN2-Tg myocytes: in $HCN3^{-/-}$ myocytes, APD was shortened by

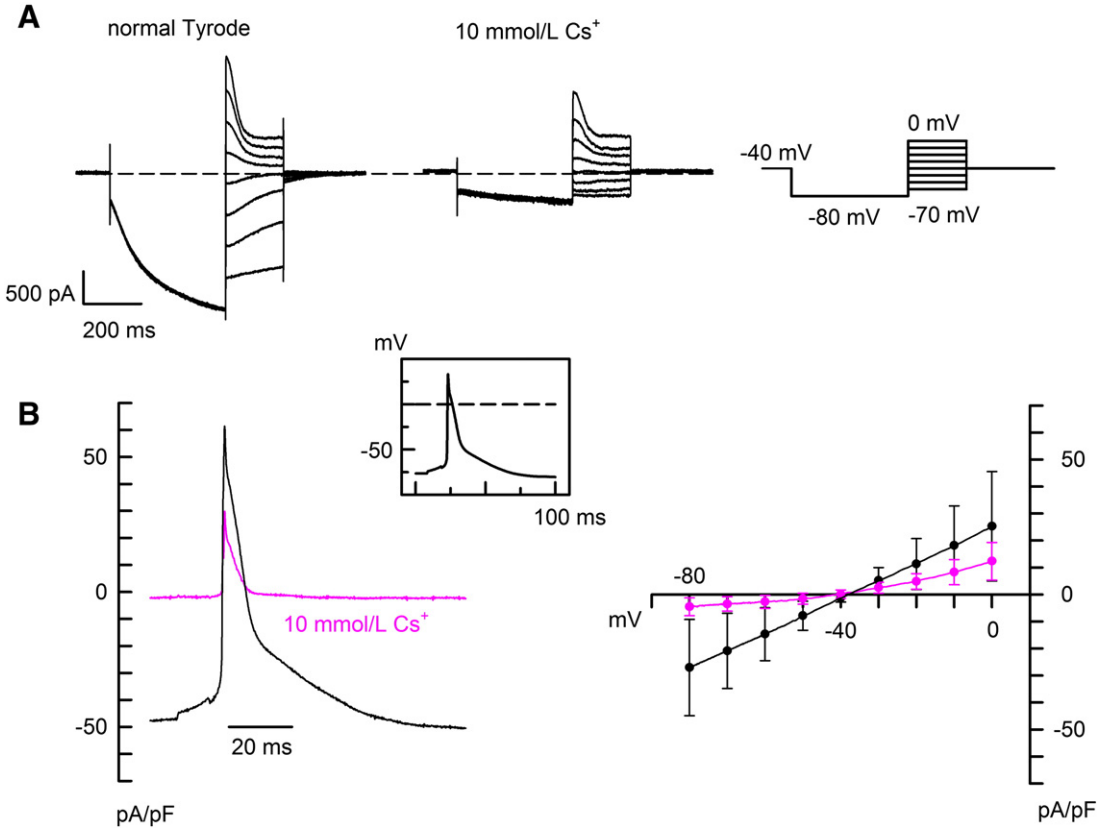

Fig. 7. Contribution of I_h tail currents to the repolarization phase of induced APs (A) HCN2 channels heterologously expressed in CHO cells were activated using a square pulse protocol (shown in the right panel). Family of I_h current before (left) and after (center) the application of 10 mmol/L Cs^+. The pipette solution contained 1 mmol/L cAMP. Note that the direction of the tail current reversed between −30 and −40 mV. (B) AP-shaped command pulses (inset) were applied to HCN2-expressing CHO cells at 0.5–5 Hz. The AP shape was sampled from HCN2-Tg myocytes in the presence of 0.3 μmol/L ISO. Left: the black trace depicts the membrane current recorded in control PBS; magenta, in 5.4 mmol/L K^+ 10 mmol/L Cs^+ bathing solution. Right: *I–V* relationship for the HCN2 current (black line) reconstructed from the repolarization phase of the AP clamp experiment in the left panel. The magenta line, recorded in 5.4 mmol/L K^+, 10 mmol/L Cs^+ bathing solution.

the reduction of inward I_h tail current at the membrane potentials more negative than −35 mV [14]. In our earlier report, this phenomenon may have been underestimated because we recorded the APs using the perforated patch method [10]. With that method, the Na^+-Ca^{2+} exchanger current driven by the intracellular Ca^{2+} transient reportedly affects the plateau phase of mouse ventricular APs at around −40 mV and might have masked the prolongation of APD in HCN2-Tg hearts [29]. It should be noted, however, that when the perforated patch method was used in mouse TAC experiments, ventricular I_h density was significantly increased and APD was significantly prolonged [13]. Reduction in repolarization reserve caused by I_h appears to be dependent on the time course of the I_h deactivation upon depolarization. Among the HCN subtypes, the order of the deactivation times at −60 mV was HCN3 > HCN4 > HCN1 > HCN2 [14]. In the present study, even HCN2, which possesses the fastest deactivation time, stayed open during the AP clamp experiments. In the hypertrophied hearts of larger animals, the expression of HCN2 and HCN4 is reportedly up-regulated [30]. Since HCN channels form heteromultimers, it would seem reasonable to expect that the time course of I_h deactivation in hypertrophied hearts would be intermediate, between those of HCN2 and HCN4, and would reduce the repolarization reserve in larger animals, whose cardiac myocytes exhibit longer APDs.

HCN channels reportedly possess Ca^{2+} permeability and re-expression of HCN channels may increase Ca^{2+} influx in hypertrophied heart [16]. The depolarization of RMP may also decrease driving force of Na^+/Ca^{2+} exchanger, thereby increasing intracellular Ca^{2+} concentration. Therefore, the pharmacological blockade of I_h may exert anti-arrhythmogenic effect by maintaining intracellular Ca^{2+} handling as well as repolarization reserve in hypertrophied heart [31].

5. Conclusions

Our findings demonstrate that the transgenic overexpression of HCN2 in the heart induces ectopic automaticity under β-adrenergic stimulation. The overexpression of HCN2 also reduces the repolarization reserve of the AP and prolongs APD. These results suggest that among fetal type cardiac channels re-expressed in heart failure, HCN2 alone is not sufficient to induce lethal arrhythmia, but it increases arrhythmogenic potential. Pharmacological blockade of HCN channels may therefore reduce the vulnerability of heart failure patients to ventricular arrhythmia.

5.1. Limitation of study

Plateau phase of mouse ventricular action potential is at ~−40 mV and is affected by intracellular Ca^{2+} transient. We therefore used Ca^{2+} buffering condition in order to evaluate the change of repolarization reserve in HCN2-Tg myocytes. On the other hand, HCN2 reportedly possesses Ca^{2+} permeability, which may potentially affect intracellular Ca^{2+} transient, giving rise to DADs and ventricular arrhythmia. This arrhythmogenic mechanism may be underestimated in the present study.

Disclosures

None declared.

Acknowledgments

We thank Ms. Hideko Yoshitake and Ms. Akemi Sakamoto for their secretarial work and Ms. Chiemi Sugiyama for her technical support.

This work was supported by a Grant-in-Aid for Scientific Research (B) from the Japan Society for the Promotion of Science (JSPS KAKENHI Grand Number 24300145) and a grant from the Ishibashi Foundation for the Promotion of Science.

Appendix A. Supplementary data

Supplementary data to this article can be found online at http://dx.doi.org/10.1016/j.yjmcc.2014.12.019.

References

[1] Wahl-Schott C, Biel M. HCN channels: structure, cellular regulation and physiological function. Cell Mol Life Sci 2009;66:470–94.
[2] Bucchi A, Baruscotti M, Robinson RB, DiFrancesco D. Modulation of rate by autonomic agonists in SAN cells involves changes in diastolic depolarization and the pacemaker current. J Mol Cell Cardiol 2007;43:39–48.
[3] Yasui K, Liu W, Opthof T, Kada K, Lee JK, Kamiya K, et al. I_f current and spontaneous activity in mouse embryonic ventricular myocytes. Circ Res 2001;88:536–42.
[4] Niwa N, Yasui K, Opthof T, Takemura H, Shimizu A, Horiba M, et al. $Ca_v3.2$ subunit underlies the functional T-type Ca^{2+} channel in murine hearts during the embryonic period. Am J Physiol Heart Circ Physiol 2004;286:H2257–63.
[5] Tomaselli GF, Beuckelmann DJ, Calkins HG, Berger RD, Kessler PD, Lawrence JH, et al. Sudden cardiac death in heart failure. The role of abnormal repolarization. Circulation 1994;90:2534–9.
[6] Nakayama H, Bodi I, Correll RN, Chen X, Lorenz J, Houser SR, et al. α1G-dependent T-type Ca^{2+} current antagonizes cardiac hypertrophy through a NOS3-dependent mechanism in mice. J Clin Invest 2009;119:3787–96.
[7] Wei-qing H, Qing-nuan K, Lin X, Cheng-hao G, Qi-yi Z. Expression of hyperpolarization-activated cyclic nucleotide-gated cation channel (HCN4) is increased in hypertrophic cardiomyopathy. Cardiovasc Pathol 2011;20:110–3.
[8] Fernández-Velasco M, Goren N, Benito G, Blanco-Rivero J, Boscá L, Delgado C. Regional distribution of hyperpolarization-activated current (I_f) and hyperpolarization-activated cyclic nucleotide-gated channel mRNA expression in ventricular cells from control and hypertrophied rat hearts. J Physiol 2003;553:395–405.
[9] Kuwahara K, Saito Y, Takano M, Arai Y, Yasuno S, Nakagawa Y, et al. NRSF regulates the fetal cardiac gene program and maintains normal cardiac structure and function. EMBO J 2003;22:6310–21.
[10] Kuwabara Y, Kuwahara K, Takano M, Kinoshita H, Arai Y, Yasuno S, et al. Increased expression of HCN channels in the ventricular myocardium contributes to enhanced arrhythmicity in mouse failing hearts. J Am Heart Assoc 2013;2:e000150-e.
[11] Oshita K, Igata S, Kuwabara Y, Kuwahara K, Ushijima K, Takano M. Isoproterenol-induced spontaneous action potentials in the cardiac myocytes of transgenic mouse overexpressing HCN2. J Physiol Sci 2013;63:S134.
[12] Takano M, Kinoshita H, Shioya T, Itoh M, Nakao K, Kuwahara K. Pathophysiological remodeling of mouse cardiac myocytes expressing dominant negative mutant of neuron restrictive silencing factor. Circ J 2010;74:2712–9.
[13] Hofmann F, Fabritz L, Stieber J, Schmitt J, Kirchhof P, Ludwig A, et al. Ventricular HCN channels decrease the repolarization reserve in the hypertrophic heart. Cardiovasc Res 2012;95:317–26.
[14] Fenske S, Mader R, Scharr A, Paparizos C, Cao-Ehlker X, Michalakis S, et al. HCN3 contributes to the ventricular action potential waveform in the murine heart. Circ Res 2011;109:1015–23.
[15] Kapoor N, Liang W, Marbán E, Cho HC. Direct conversion of quiescent cardiomyocytes to pacemaker cells by expression of Tbx18. Nat Biotechnol 2013;31:54–62.
[16] Yu X, Chen X-W, Zhou P, Yao L, Liu T, Zhang B, et al. Calcium influx through I_f channels in rat ventricular myocytes. Am J Physiol Cell Physiol 2007;292:1147–55.
[17] Stillitano F, Lonardo G, Zicha S, Varro A, Cerbai E, Mugelli A, et al. Molecular basis of funny current (I_f) in normal and failing human heart. J Mol Cell Cardiol 2008;45:289–99.
[18] Hoppe UC, Jansen E, Südkamp M, Beuckelmann DJ. Hyperpolarization-activated inward current in ventricular myocytes from normal and failing human hearts. Circulation 1998;97:55–65.
[19] Jaleel N, Nakayama H, Chen X, Kubo H, MacDonnell S, Zhang H, et al. Ca^{2+} influx through T- and L-type Ca^{2+} channels have different effects on myocyte contractility and induce unique cardiac phenotypes. Circ Res 2008;103:1109–19.
[20] Boink GJJ, Duan L, Nearing BD, Shlapakova IN, Sosunov EA, Anyukhovsky EP, et al. HCN2/SkM1 gene transfer into canine left bundle branch induces stable, autonomically responsive biological pacing at physiological heart rates. J Am Coll Cardiol 2013;61:1192–201.
[21] Kinoshita H, Kuwahara K, Takano M, Arai Y, Kuwabara Y, Yasuno S, et al. T-type Ca^{2+} channel blockade prevents sudden death in mice with heart failure. Circulation 2009;120:743–52.
[22] Galindo CL, Skinner MA, Errami M, Olson LD, Watson DA, Li J, et al. Transcriptional profile of isoproterenol-induced cardiomyopathy and comparison to exercise-induced cardiac hypertrophy and human cardiac failure. BMC Physiol 2009;9:23.
[23] Adachi T, Shibata S, Okamoto Y, Sato S, Fujisawa S, Ohba T, et al. The mechanism of increased postnatal heart rate and sinoatrial node pacemaker activity in mice. J Physiol Sci 2013;63:133–46.
[24] Nerbonne JM, Kass RS. Molecular physiology of cardiac repolarization. Physiol Rev 2005;85:1205–53.
[25] Ishihara K, Yan DH, Yamamoto S, Ehara T. Inward rectifier K^+ current under physiological cytoplasmic conditions in guinea-pig cardiac ventricular cells. J Physiol 2002;540:831–41.
[26] Babij P, Askew GR, Nieuwenhuijsen B, Su CM, Bridal TR, Jow B, et al. Inhibition of cardiac delayed rectifier K^+ current by overexpression of the long-QT syndrome HERG G628S mutation in transgenic mice. Circ Res 1998;83:668–78.

[27] Nattel S, Maguy A, Le Bouter S, Yeh YH. Arrhythmogenic ion-channel remodeling in the heart: heart failure, myocardial infarction, and atrial fibrillation. Physiol Rev 2007;87:425–56.
[28] Varró A, Baczkó I. Cardiac ventricular repolarization reserve: a principle for understanding drug-related proarrhythmic risk. Br J Pharmacol 2011;164:14–36.
[29] Wang J, Chan TO, Zhang XQ, Gao E, Song J, Koch WJ, et al. Induced overexpression of Na^+/Ca^{2+} exchanger transgene: altered myocyte contractility, $[Ca^{2+}]_i$ transients, SR Ca^{2+} contents, and action potential duration. Am J Physiol Heart Circ Physiol 2009; 297:H590–601.
[30] Herrmann S, Stieber J, Ludwig A. Pathophysiology of HCN channels. Pflugers Arch 2007;454:517–22.
[31] Swedberg K, Komajda M, Böhm M, Borer JS, Ford I, Dubost-Brama A, et al. Ivabradine and outcomes in chronic heart failure (SHIFT): a randomised placebo-controlled study. Lancet 2010;376:875–85.